S. Sun, G. R. MacCartney, M. K. Samimi, S. Nie, and T. S. Rappaport, "Millimeter wave multi-beam antenna combining for 5G cellular link improvement in New York City," in *Communications (ICC), 2014 IEEE International Conference on*, June 2014, pp. 5468-5473.

Millimeter Wave Multi-beam Antenna Combining for 5G Cellular Link Improvement in New York City

Shu Sun*, George R. MacCartney Jr., Mathew K. Samimi, Shuai Nie and Theodore S. Rappaport*
NYU WIRELESS
Polytechnic School of Engineering, New York University, Brooklyn, NY 11201
*Corresponding Email: ss7152@nyu.edu, tsr@nyu.edu

***Abstract*—The performance of multi-beam antenna equal gain combining for improving signal quality in future millimeter-wave cellular systems is evaluated in this article. Employing experimental data obtained from 28 GHz and 73 GHz propagation measurements in the dense urban environment of New York City, we present the impact of coherent bi-beam, tri-beam and quad-beam combining on path loss and shadow factors. The results reveal that a maximum of 24.9 dB improvement in path loss at 28 GHz and 34.8 dB at 73 GHz for 100 m T-R (transmitter-receiver) separation distances can be achieved via combining the strongest four received signals from distinct beams, when compared to the case of signals at the receiver with randomly pointed beams. Comparable path loss values are achieved at both 28 and 73 GHz bands. This paper demonstrates the potential of utilizing spatial filtering and beam combining to significantly improve received signal levels and link margins at millimeter-wave frequencies.**

Keywords—Equal gain combining; beam combining; millimeter wave; 28 GHz; 73 GHz; 5G

I. INTRODUCTION

Diversity is a powerful communication technique that can reduce the detrimental effects of signal fading on wireless communication system performance. Diversity can improve signal outage, average bit error rate (BER), and signal-to-noise ratio (SNR) by using two or more communication channels with different characteristics [1].A variety of diversity schemes exist, such as time diversity, frequency diversity, space diversity and polarization diversity, all of which may provide significant link budget and signal quality improvement. Space diversity, also known as a special type of antenna diversity, is one of the most effective implementations of diversity utilized in wireless communication systems. A wide range of space diversity reception techniques can be distinguished: selection diversity (SD), feedback diversity (FD), maximal ratio combining (MRC) and equal gain combining (EGC).

MRC yields the optimal statistical reduction of fading of any known linear diversity combiner, but it requires the knowledge of phase and amplitude of the signals, which complicates the implementation mechanism. In comparison, EGC merely needs the estimation of phase information, which leads to a less complex implementation in practice [2][3], thus it is widely employed. The performance assessment of EGC with equal power co-channel interference is reported in [4], whereas [5] analyzed the error probability of EGC with quantized channel phase compensation in Rice and Hoyt fading channels. The performance of EGC receivers in generalized fading channels has also been explored [6], and recently an approximate expression for BER using EGC in multicarrier code-division multiple-access (MC-CDMA) systems was achieved [7]. While research works on EGC abound, most of them focus on the theoretical error and SNR analysis without thorough experimental data, and most research has used well-known conventional channel models that assume omnidirectional antennas.

In addition to the preceding diversity techniques, beamforming is also an effective technique to improve received signal quality. Coupled with Multiple-Input Multiple-Output (MIMO) systems using antenna arrays, beamforming can substantially increase the signal-to-interference and noise ratio (SINR) at the desired user by creating corresponding antenna patterns. Extensive research work has been done to explore diverse beamforming approaches for different architectures and environments [8-10]. If beam combining is implemented following beamforming, then the signal level and link margin may be further improved.

As millimeter wave (mmWave) systems proliferate, the use of spatial filtering and diversity combining at mmWave frequencies becomes an attractive research field. In this paper, we demonstrate the multi-beam combining results using EGC based on data obtained from extensive urban propagation measurements using rotatable horn antennas in the densely populated environment of New York City at two mmWave bands: 28 GHz [11-13] and 73 GHz [14][15]. These frequencies are in the Ka-band and E-band, respectively, and are prospective candidates for fifth generation (5G) wireless communication systems in dense urban environments.

II. EXPERIMENTAL PROCEDURE

A. Measurement Procedure

To mimic small cell deployments of future mmWave systems, comprehensive measurements were taken in urban canyon environments. 28 GHz outdoor propagation

measurements were conducted using three TX locations (with heights of 7m, 7m, 17m, respectively) and 25 RX locations (generating 75 TX-RX location combinations) around the NYU campus in downtown New York City, in the summer of 2012, utilizing a spread spectrum sliding correlator channel sounder with an 800 MHz first null-to-null RF bandwidth and a multipath time resolution of 2.5 ns. 24.5 dBi (10.9^0 half-power beamwidth) vertically polarized steerable directional horn antennas were employed at both the TX and RX. At each RX location, ten antenna pointing angle configurations (a configuration denotes a particular elevation and azimuth angle convention for the TX and RX antennas) were utilized, and extensive measurements were carried out for each configuration. Details of the measurement procedure are provided in [8].

In the summer of 2013, a similar sliding correlator channel sounder was used for the 73 GHz outdoor measurement campaign in downtown Manhattan around the NYU campus. Measurements were conducted using five TX locations and 27 RX locations, where a pair of 27 dBi (7^0 half-power beamwidth) vertically polarized steerable horn antennas was used at the TX and RX. Two TX sites were located on the Coles Sports Center building rooftop (7 m above ground level), another two TX sites were on the 2nd-floor balcony of the Kimmel center of NYU (7 m relative to ground), and another TX site was on the fifth-story balcony of the Kaufman Business School (17 m above ground level). For each TX location, a number of RX locations, separated from the TX within 200 meters, were chosen. Two types of measurement scenarios were performed at most of the RX locations: 1) base station-to-mobile scenario where the RX antenna height is 2 m, and 2) backhaul-to-backhaul scenario where the RX antenna height is 4.06 m (lamppost height), that yielded 36 TX-RX location combinations for mobile and 38 for backhaul. A pneumatic mast was used to adjust the height of the receiver antenna.

For each TX-RX location combination and scenario, the TX and RX horn antennas were mechanically rotated in both the azimuth and elevation planes to exhaustively search for the strongest received power angle combinations. For the strongest received power angle combination identified, the RX antenna was then swept over 360^0 in 10^0 or 8^0 increments (depending on the environment) in the azimuth plane with the TX antenna fixed in both the azimuth and elevation plane. At each increment, a power delay profile (PDP) was recorded at the RX where a signal could be acquired. Then, the RX elevation was fixed to uptilt/downtilt one beamwidth for two RX sweeps, followed by the TX elevation being fixed to uptilt/downtilt one beamwidth for another two RX sweeps, resulting in five initial RX sweeps. Afterwards, TX sweeps were conducted with the RX antenna fixed in the two strongest azimuth and elevation angle combinations determined during the first five RX sweeps. Following the two TX sweeps, another main angle of departure at the TX was selected to perform five additional RX sweeps, similar to the first five. This resulted in up to 12 possible measurement sweeps per TX-RX location combination for an individual scenario (mobile or backhaul).

Measurements were conducted in both line-of-sight (LOS) and non-line-of-sight (NLOS) environments. In the LOS environment, the TX and RX antennas were perfectly pointed at each other boresight-to-boresight. In the NLOS environment, the TX and RX antennas were blocked by obstructions or were not aligned boresight-to-boresight, even if there was an optical path. Since there was merely one signal (i.e. one beam) in the LOS environment for each TX-RX location combination, beam combining was only considered for NLOS environments.

Fig. 1 shows a typical polar plot displaying the azimuth angles of arrival (AOAs) at one RX in a NLOS environment at 73 GHz. The 0^0 azimuth pointing angle refers to true north. The rotation step was 8^0. As is observed, power was received at 26 out of 45 RX azimuth angles, implying that downtown Manhattan is a multipath-rich environment with numerous reflective objects and that signals coming from a myriad of beams can be combined to enhance the received signal level. At all 26 TX-RX location combinations in the 28 GHz measurements and 62 TX-RX location and scenario combinations for 73 GHz where signals were received, at least four distinct signals coming from different directions were obtained at each single location combination by measuring various azimuth and elevation angles.

B. Beam Combining Procedure

Beam combining at 28 GHz using the floating intercept model has been studied in [16], while the close-in free space reference distance path loss model is adopted in this work. The equal gain coherent beam combining procedure was employed, where the square root of the absolute (i.e. linear) received power levels in Watts (i.e. the total received power in the power delay profile (PDP)) were computed, and the voltages (i.e. square root of power) obtained at the strongest few 3D (three dimensional) antenna pointing angles in post processing were summed, hence the total coherent voltage was found at each RX location. This value was then squared to obtain received power in units of Watts, which was finally converted back into dBm. Eqs. (1) and (2) show the methods of calculating the total received coherent (P_C) and noncoherent (P_{NC}) powers at each RX using the combination of the N strongest beams based on the powers in PDPs, respectively:

$$P_C = (\sum_{i=1}^{N} \sqrt{P_i})^2 \quad (1)$$

$$P_{NC} = \sum_{i=1}^{N} P_i \quad (2)$$

where P_C and P_{NC} denote the coherently and noncoherently combined powers in Watts, respectively. P_i (i=1,2,…, N) represents the i^{th} strongest received power (in Watts). By using the resulting received power from beam combining, the corresponding path loss was computed. This work does not address arrival time alignment of different beams at each RX, but focuses on theoretical analysis.

The path loss exponent (PLE) is a parameter commonly used to describe the attenuation of a signal as it propagates

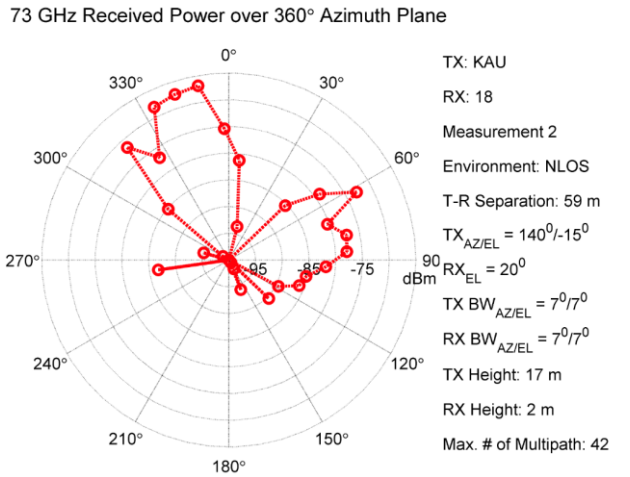

Fig. 1. Polar plot showing the received powers at a NLOS location at 73 GHz with TX heights of 17 m and RX heights of 2 m and 59 m TX-RX separation. The red dots represent total received powers in dBm at different RX azimuth pointing angles.

in the channel. In previous works [13][15], a floating intercept model was employed to characterize path loss. The slope of the LMS (least mean squares) fitted line in that model, however, does not have a clear physical meaning, while the slope in the close-in free space reference model represents the PLE which is quite useful in analyzing the channel properties based on a realistic free space reference. Thus the close-in free space reference model is adopted here. Path loss at a close-in reference distance d_0 in meters is calculated as the free space path loss by Eq. (3):

$$PL(d_0) = 20log_{10}\left(\frac{4\pi d_0}{\lambda}\right) \quad (3)$$

where λ is the wavelength of the carrier frequency, which equals 10.71 mm at 28 GHz and 4.08 mm at 73.5 GHz. Without loss of generality, in our measurements d_0 is set to 4 m, which is much larger than the Fraunhofer distances for our antennas at both frequencies. Path loss at a T-R separation d in meters, beyond d_0, is given by the equation below [1]:

$$PL(d) = PL(d_0) + 10nlog_{10}\left(\frac{d}{d_0}\right) + X_\sigma \quad (4)$$

where $PL(d)$ is the path loss in dB for a T-R separation of d in meters, n is the path loss exponent, and X_σ is a Gaussian random variable with a mean of 0 dB and standard deviation of σ in dB, also known as the shadow factor (SF).

III. Results And Analysis

A. 28 GHz Measurements

Fig. 2 illustrates the path loss measured with a 7m-high TX antenna on the roof of Coles Sports Center for the NLOS environment. The overall PLEs for NLOS for all possible RX antenna pointing angles is 5.42 with a SF of 10.39 dB, implying the tough urban environment for millimeter waves to propagate in. But when only considering the best beam at each RX site, the PLE is

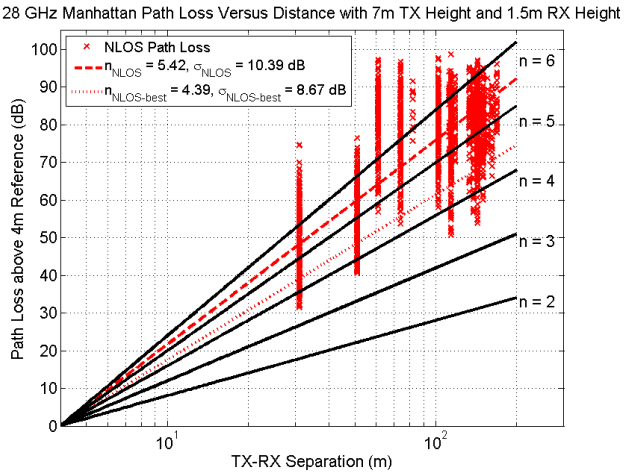

Fig. 2. Measured path loss values relative to 4 m free space path loss for 28 GHz outdoor cellular channels. These path loss values were measured using 24.5 dBi narrow beam antennas for 16 NLOS TX-RX location combinations with TX heights of 7 m and RX heights of 1.5 m. The values in the legend represent the PLEs and shadow factors, where NLOS-best represents the single best RX pointing angle at each location combination.

reduced to 4.39 with a SF of 8.67 dB. The beam combining results for NLOS are shown in Fig. 3. Note that the PLE becomes lower after beam combining and keeps decreasing with the increasing number of combined beams, e.g., the PLE drops from 4.39 (using the single best beam at the RX) to 4.00 when the best two signals are coherently combined, and becomes 3.64 when combining the strongest four signals in a coherent way at the RX. Furthermore, the performance of coherent combining is superior to that of non-coherent combining. For instance, the improvement in PLE by coherently combining *two* beams is even more substantial than by non-coherently combining *four* beams. It is also worth mentioning that the shadow factors are always lower after beam combining compared to the path loss values where all possible pointing angles are considered.

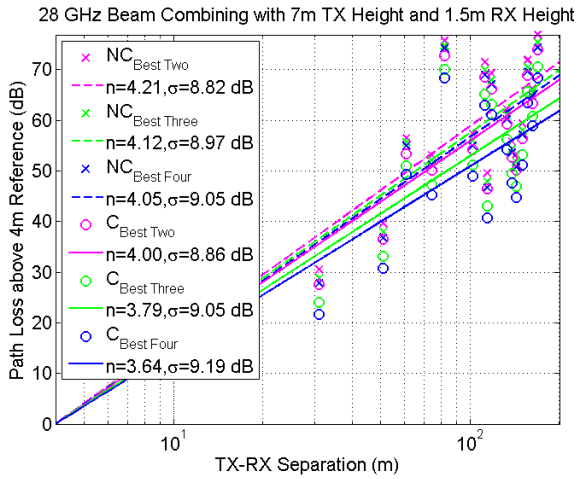

Fig. 3. Path loss versus T-R separation at 28 GHz in NYC for the best (i.e. strongest) two, three and four beams combined noncoherently and coherently at each RX location for 16 NLOS TX-RX location combinations with TX heights of 7 m and RX heights of 1.5 m. The values in the legend represent the PLEs and shadow factors for each kind of beam combination, "NC" denotes non-coherent combining, and "C" means coherent combining.

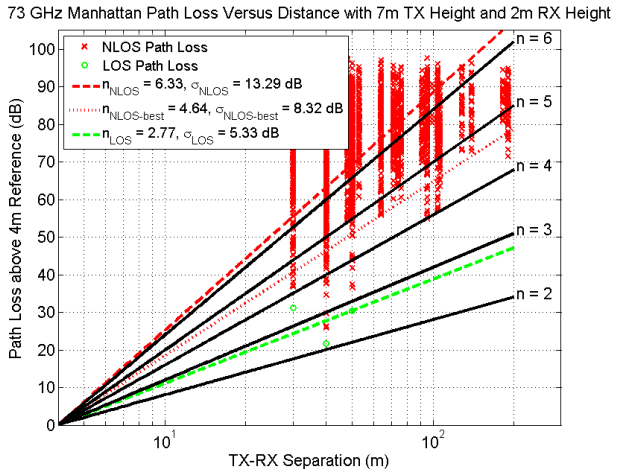

Fig. 4. Measured path loss values relative to 4 m free space path loss for 73 GHz outdoor cellular channels. These path loss values were measured using 27 dBi narrow beam antennas for 19 TX-RX location combinations with TX heights of 7 m and RX heights of 2 m. The values in the legend represent the PLEs and shadow factors, where NLOS-best represents the single best RX pointing angle at each location combination.

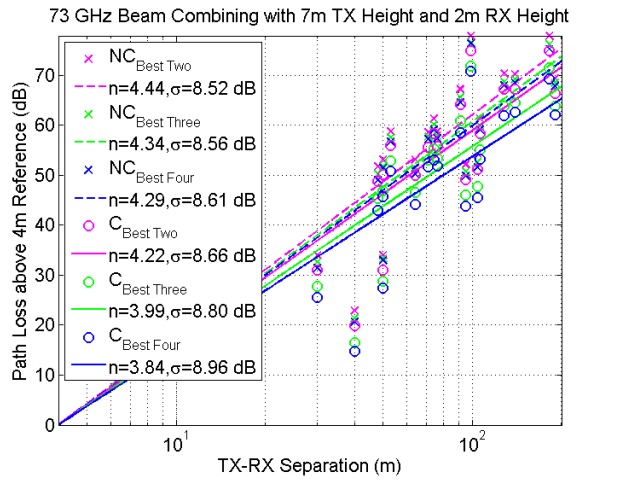

Fig. 5. Path loss versus T-R separation at 73 GHz in NYC for the best (i.e. strongest) two, three and four beams combined noncoherently and coherently at each RX location for 19 NLOS TX-RX location combinations with TX heights of 7 m and RX heights of 2 m. The values in the legend represent the PLEs and shadow factors for each kind of beam combination, "NC" denotes non-coherent combining, and "C" means coherent combining.

The PLEs and corresponding SFs with the TX at 17 m above ground on the fifth-story balcony of Kaufman Business School at 28 GHz can be found in Table 1. It is obvious that the PLEs are generally a bit lower for the TX with a height of 7 m than the 17 m case, but the discrepancies are not large.

B. 73 GHz Measurements

Fig. 4 shows the path loss values obtained from all measurements over all pointing angles for a 7 m TX height at 73 GHz. The PLE for the entire NLOS environment is 6.33, which reduces to 4.64 when using just the single strongest pointing direction at each location combination. The PLE for LOS is 2.77, which is higher than the theoretical value 2.0, the reason lies in that in our LOS

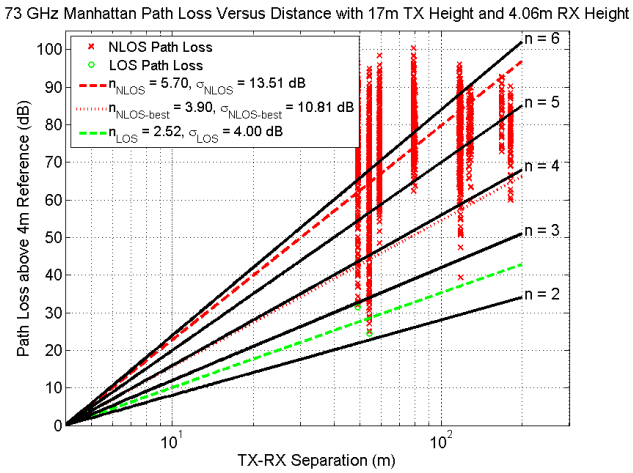

Fig. 6. Measured path loss values relative to 4 m free space path loss for 73 GHz outdoor cellular channels. These path loss values were measured using 27 dBi narrow beam antennas for 11 TX-RX location combinations with TX heights of 17 m and RX heights of 4.06 m. The values in the legend represent the PLEs and shadow factors, where NLOS-best represents the single best RX pointing angle at each location combination.

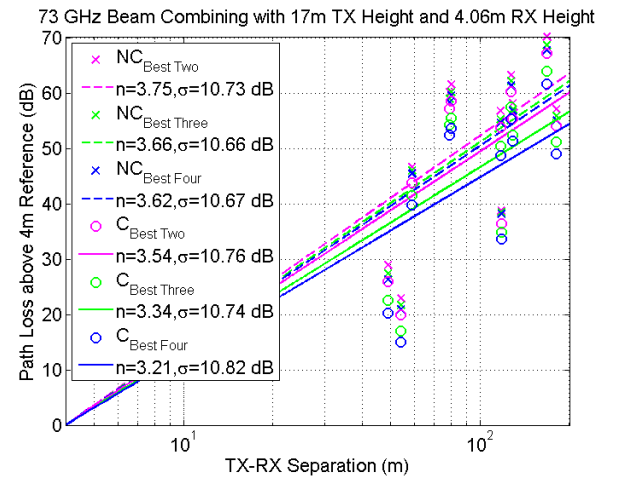

Fig. 7. Path loss versus T-R separation at 73 GHz in NYC for the best (i.e. strongest) two, three and four beams combined noncoherently and coherently at each RX location for 11 NLOS TX-RX location combinations with TX heights of 17 m and RX heights of 4.06 m. The values in the legend represent the PLEs and shadow factors for each kind of beam combination, "NC" denotes non-coherent combining, and "C" means coherent combining.

definition, the TX and RX antennas are facing each other boresight-to-boresight, but it is difficult to perfectly align the antennas boresight-to-boresight at such large distances, thus the PLE increases. Fig. 5 displays the corresponding beam combining outcomes for 73 GHz. After implementing four-beam combining, as is shown in Fig. 5, the PLE descends to 3.84, much more favorable for propagation.

Figs. 6 and 7 demonstrate the behavior of PLEs and shadow factors before and after coherent multi-beam combining for the backhaul-to-backhaul scenario with the TX antennas 17m high and the RX antennas 4.06m high at 73 GHz. It is clear from these figures that combining the few strongest signals can tremendously raise signal quality and reduce the PLEs , thus improving the link budget and

Table 1. Path loss exponents (PLEs) with respect to 4 m free space references and standard deviations (or shadow factors) at both 28 GHz and 73 GHz for various transmitter and receiver heights and different propagation scenarios. The beam combining results are obtained using the coherent combining scheme. At each TX-RX location combination, at least four unique beams are obtained and all beams use the square root of power from the PDP for coherent power combining.

Frequency (GHz)	TX, RX Antenna Gains (dBi)	TX-RX Separation Range (m)	TX Height (m)	RX Height (m)	Path Loss Scenarios (Using Coherent Beam Combining)		Path Loss Exponent (PLE)	σ_{SF} (dB)
28 GHz New York City	+24.5, +24.5 both vertically polarized	30 ~ 200	7	1.5	Non-line-of-sight (NLOS)	Overall	5.42	10.39
						Best One	4.39	8.67
						Best Two	4.00	8.86
						Best Three	3.79	9.05
						Best Four	3.64	9.19
			17	1.5	Non-line-of-sight (NLOS)	Overall	5.33	8.83
						Best One	4.56	7.89
						Best Two	4.17	8.21
						Best Three	3.95	8.44
						Best Four	3.80	8.62
73 GHz New York City	+27, +27 both vertically polarized	30 ~ 200	7	4.06	Line-of-sight (LOS)		2.68	6.79
					Non-line-of-sight (NLOS)	Overall	6.06	14.44
						Best One	4.72	9.52
						Best Two	4.33	9.51
						Best Three	4.12	9.51
						Best Four	3.98	9.51
				2	Line-of-sight (LOS)		2.77	5.33
					Non-line-of-sight (NLOS)	Overall	6.33	13.29
						Best One	4.64	8.32
						Best Two	4.22	8.66
						Best Three	3.99	8.80
						Best Four	3.84	8.96
			17	4.06	Line-of-sight (LOS)		2.52	4.00
					Non-line-of-sight (NLOS)	Overall	5.70	13.51
						Best One	3.90	10.81
						Best Two	3.54	10.76
						Best Three	3.34	10.74
						Best Four	3.21	10.82
				2	Line-of-sight (LOS)		2.32	2.71
					Non-line-of-sight (NLOS)	Overall	5.52	12.86
						Best One	3.76	8.81
						Best Two	3.39	8.89
						Best Three	3.19	8.87
						Best Four	3.05	8.87

extending the transmitter's coverage area.

The PLEs and shadow factors with and without multi-beam combining for other TX and RX heights at 73 GHz are provided in Table 1. It can be summarized from the table that the PLEs are generally lower when the height of TX antenna is raised, while the RX antennas are of the same height. This is because when the TX antenna is raised, the emitted signal usually encounters fewer obstructions which may block the path or absorb its energy as it propagates in the channel, thus would be less attenuated. This implies the possibility of obtaining better signal quality by increasing the TX antenna height at 73 GHz.

As coherent beam combining offers improvement in the received signal quality and link budget, it is desirable to utilize this method in cellular communication systems. One approach of achieving beam combining gain is using RAKE receivers that combine the multipath components from multiple fingers. Since RAKE combiners require training symbols to estimate the channel impulse response, the receiver complexity is high thus suggesting frequency-domain techniques.

C. Comparison of 28 GHz and 73 GHz Measurements

The contrast of the PLEs and shadow factors in different scenarios between 28 GHz and 73 GHz carrier frequencies is also shown in Table 1. Without beam combining, when comparing the PLEs in base station-to-mobile scenarios at both frequencies, where the RX antenna height is 1.5 m at 28 GHz and 2 m at 73 GHz, it can be seen that the overall PLEs in NLOS situations are smaller at 28 GHz than at 73 GHz. The PLEs at both 28 GHz and 73 GHz are around 5 or 6 for the overall received beams in any direction, and around 4 or 4.5 for the best single beam pointing angle, indicating that the path loss values are comparable for the same TX heights and similar RX heights. These observations suggest that there is no definite relationship between path loss and the carrier frequency in the mmWave range in a densely populated urban environment like New York City. It is evident from the 8th column in Table 1 that the PLE for a certain propagation condition exhibits the same trend at both 28 GHz and 73 GHz, i.e. it drops considerably after multi-beam combining is performed, and decreases monotonically as the number of combined signals increases. For instance, the PLE corresponding to four coherently combined signals in a NLOS environment with 7 m TX heights and 2 m RX heights at 73 GHz declined by

2.49 and 0.80 compared to that before beam combining, and that of using the single best beam, respectively. Considering a T-R separation of 100 m for which the PLE decreases from 6.33 to 3.84, the equivalent path loss drops by about 34.8 dB, and 11.2 dB for the case when PLE descends from 4.64 (corresponding to the best single beam) to 3.84, which is a remarkable improvement in link budget, and quite significant to carriers. Similarly, path loss can be reduced by up to 24.9 dB for 100 m T-R separation at 28 GHz contrasting the result of combining four beams and that without beam combining. These improvements can be easily found based on Eq. (4) by using $d_0 = 4\,m, d = 100\,m$, and comparing the path loss values for the two different PLEs.

IV. CONCLUSION

The striking effect of coherent multi-beam combining at the mobile receiver antenna on PLEs and link quality at both 28 GHz and 73 GHz carrier frequencies has been demonstrated. The results show that beam combining can significantly reduce PLEs (e.g. from 6.33 to 3.84) and shadow factors (e.g. from 13.29 to 8.96), thus improving received signal quality and extending link coverage. In particular, combining the four strongest signals yields about 34.8 dB of link enhancement over a single arbitrarily pointed beam, and more than 11.2 dB of improvement when compared to a single optimum beam over a 100 m TX-RX separation at 73 GHz. The maximum possible improvement on received power at 28 GHz reaches 24.9 dB. Measurements showed that path loss exhibited similar values at both frequencies. This work reveals the potential of using smart antennas to exploit the spatial degrees of freedom in the propagation channel and ameliorate link margin in future wireless communication systems. Work is now needed to implement broadband beam combining for mmWave systems.

ACKNOWLEDGMENT

The 28 GHz campaign was sponsored by Samsung DMC R&D Communications Research Team (CRT) through Samsung Telecommunications America, LLC. The 73 GHz campaign was sponsored by Nokia Solutions and Network (NSN) and the GAANN Fellowship program. The authors wish to thank Hannar J. Lee, Abhi Shah and Rimma Mayzus of NYU WIRELESS for their contributions to the projects, and the NYU Administration, NYU Public Safety, and the NYPD for their support of the measurement campaigns. The projects were also supported by the following NYU WIRELESS Industrial Affiliates: Samsung, National Instruments, Qualcomm, NSN, L-3 Communications, Huawei, AT&T, and Intel.

REFERENCES

[1] T. S. Rappaport, Wireless Communications: Principles and Practice, 2nd Edition, New Jersey: Prentice Hall, pp. 380&139, 2002.

[2] H. O. Peterson, H. H. Beverage, "Diversity receiving system of RCA communications" Proc. IRE, vol.42, pp.531-561, April 1931.

[3] D. G. Brennan, "Linear diversity combining techniques", *IEEE Proc.*, vol. 91, no. 2, February 2003.

[4] A. Annamalai, C. Tellambura and Vijay and K. Bhargava "Equal gain diversity receiver performance in wireless channels", *IEEE Trans. on Comm.*, vol. 48, no. 10, 2000.

[5] D. A. Zogas, G. K. Karagiannidis, and S. A. Kotsopoulos, "Equal gain combining over Nakagami-n (Rice) and Nakagami-q (Hoyt) generalized fading channels," *IEEE Trans. Wireless Commun*., vol. 4, no. 2, pp. 374–379, Mar. 2005.

[6] G. K. Karagiannidis, N. C. Sagias, and D. A. Zogas, "Error analysis of M-QAM with equal-gain diversity over generalized fading channels," *IEE Proc. On Commun*, vol. 152, no. 1, pp. 69–74, Feb. 2005.

[7] I. Develi, A. Akdagli, "Approximate expression of bit error rate in uplink MC-CDMA systems with equal gain combining," *Journal of Communications and Networks*, vol.15, no.1, pp.25,30, Feb. 2013.

[8] R. Mudumbai, D. R. Brown, U. Madhow, H. V. Poor, "Distributed transmit beamforming: challenges and recent progress," *IEEE Communications Magazine*, vol.47, no.2, pp.102-110, February 2009.

[9] C. Junil, Z. Chance, D. J. Love, U. Madhow, "Noncoherent trellis-coded quantization for massive MIMO limited feedback beamforming," *Information Theory and Applications Workshop (ITA)*, pp.1-6, 10-15 Feb. 2013.

[10] E. Torkildson, U. Madhow, M. Rodwell, "Indoor Millimeter Wave MIMO: Feasibility and Performance," *IEEE Transactions on Wireless Communications*, vol.10, no.12, pp.4150-4160, December 2011.

[11] Y. Azar, G. N. Wong, K. Wang, R. Mayzus, J. K. Schulz, H. Zhao, F. Gutierrez, D. Hwang, T. S. Rappaport, "28 GHz Propagation Measurements for Outdoor Cellular Communications Using Steerable Beam Antennas in New York City," in *2013 IEEE International Conference on Communications (ICC)*, June 9-13, 2013.

[12] T. S. Rappaport, S. Sun, R. Mayzus, H. Zhao, Y. Azar, K. Wang, G. N. Wong, J. K. Schulz, M. Samimi, F. Gutierrez, "Millimeter Wave Mobile Communications for 5G Cellular: It Will Work!," *IEEE Access*, vol.1, pp.335-349, 2013.

[13] G. R. MacCartney, J. Zhang, S. Nie, T. S. Rappaport, "Path Loss Models for 5G Millimeter Wave Propagation Channels in Urban Microcells," to appear in *2013 IEEE Global Communications Conference (GLOBECOM)*, Atlanta, GA, USA, 9-13 Dec. 2013.

[14] S. Nie, G. R. MacCartney, S. Sun, T. S. Rappaport, "72 GHz Millimeter Wave Indoor Measurements for Wireless and Backhaul Communications",in *IEEE 24th Annual International Symposium on Personal, Indoor, and Mobile Radio Communications (PIMRC)*, Sep. 8~11, 2013.

[15] M. Akdeniz, Y. Liu, S. Sun, S. Rangan, T. S. Rappaport, E. Erkip, "Millimeter Wave Channel Modeling and Cellular Capacity Evaluation," submitted to *IEEE Journal on Selected Areas in Communications (JSAC)*, Dec. 2013.

[16] S. Sun, T. S. Rappaport, "Mulit-beam Antena Combining for 28 GHz Cellular Link Improvement in Urban Environments," to appear in *2013 IEEE Global Communications Conference (GLOBECOM)*, Atlanta, GA, USA, 9-13 Dec. 2013.